


 PHOTOPRODUCTION AT LOW Q^2

P. J. BUSSEY

*Department of Physics and Astronomy,
 University of Glasgow,
 Glasgow G12 8QQ, U.K.
 E-mail: p.bussey@physics.gla.ac.uk*

Talk given at 19th *Physics in Collision* conference, Ann Arbor, USA, June 1999.

The past year has seen a number of important developments in hard photoproduction physics at the HERA collider. These are surveyed.

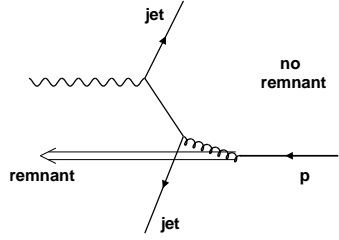
1 Introduction

The record luminosities obtained in recent years at the HERA collider have given many new results in deep inelastic scattering. However most of the virtual photons that mediate the ep collisions have low Q^2 values; these large fluxes of quasi-real photons have made HERA an outstanding laboratory in which to study photon physics. Here I survey some of the recent results reported by the experiments H1 and ZEUS, concentrating on the hard interactions which reveal the partonic structure of the photon.

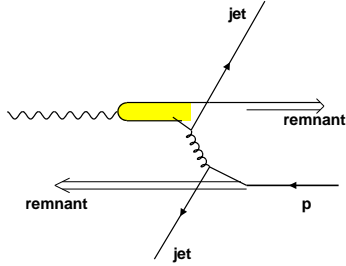
Throughout, it will be helpful to have in mind three characteristic modes by which a photon can interact with a proton at high energies. These are illustrated in fig. 1.¹ The simplest is when the entire photon couples in a pointlike manner to a high transverse energy (E_T) $q\bar{q}$ pair; such diagrams are referred to as “direct” photon processes. The photon may also couple non-perturbatively to a hadronic state which then interacts with the proton. Both the hadronic state and the proton can be sources of partons which undergo hard QCD scattering; such diagrams are known as “resolved” photon processes.

These two classes of process are fully separable only in lowest order (LO) QCD. A more complex situation occurs when the photon couples in a pointlike way to a medium- E_T $q\bar{q}$ pair, one of which then undergoes a hard scatter. Here there are three perturbative couplings and the process is no longer LO. Such processes are referred to as “anomalous”. Both pointlike and hadronic photon couplings are also present, of course, in higher order diagrams.

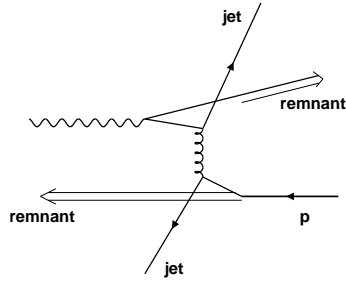
With the above theoretical ideas in the background, in practice we wish to make experimental observations. The principal measurable quantities available in hard photon reactions are high E_T jets, high E_T photons (“prompt” photons), various single particle spectra and the remnants of the incoming photon and proton. The quantities we would like to study include the nature of the outgoing quarks and gluons, and the hadronic structure of the



(a) Pointlike photon coupling to a high- E_T quark pair. There is no photon remnant. In the LO diagram illustrated, $x_\gamma = 1$.



(b) Hadronic photon coupling. The photon acts as a source of partons which can scatter off partons in the proton. There is a photon remnant as well as a proton remnant.



(c) Anomalous photon coupling. The photon couples perturbatively to a medium- E_T quark pair. There is a photon remnant at non-zero transverse momentum.

Figure 1. Schematic illustrations of photoproduction processes.

photon, in addition to the challenge of verifying that we have an adequate understanding of the basic QCD mechanisms that are operating.

A basic parton-level concept is that of x_γ , the fraction of the photon energy that takes part in the main hard QCD subprocess. (Above LO this may not always be defined simply.) In practice, what is wanted is a measurable quantity which correlates with x_γ in a chosen theoretical description of the process. For dijet final states, two such experimental estimators are

$$x_\gamma^{obs} = \frac{\Sigma_{jets} E_T^{jet} e^{-\eta^{jet}}}{2E_\gamma} \quad \text{and} \quad x_\gamma^{jets} = \frac{\Sigma_{jets} (E^{jet} - p_z^{jet})}{\Sigma_{hadr} (E^{hadr} - p_z^{hadr})}$$

which have been used by ZEUS and H1. Here as elsewhere, η denotes laboratory pseudorapidity and the proton beam defines the “forward” (+ Z) direction. ($E_T e^{-\eta} \equiv (E - p_z)$; the above formulae differ in the averaging of the parameters over the particles in the jet.) To facilitate comparisons with theory, both estimators are defined at the final-state hadron level.

In the following sections, photoproduction results will be presented on:

- (i) dijet final states
- (ii) prompt photons
- (iii) the parton content of the photon
- (iv) the photon remnant, and
- (v) properties of the final-state jet system.

2 Dijet final states.

The integrated luminosities now available from HERA allow jets to be measured out to high E_T values. This is illustrated in fig. 2(a), where the E_T spectrum seen in ZEUS² is compared to theory using several models of the photon parton density, making use of recent next-to-leading order (NLO) calculations³ whose predictions do not differ from each other on the scale of the figure. Agreement is excellent in all cases. The k_T jet algorithm is used,⁴

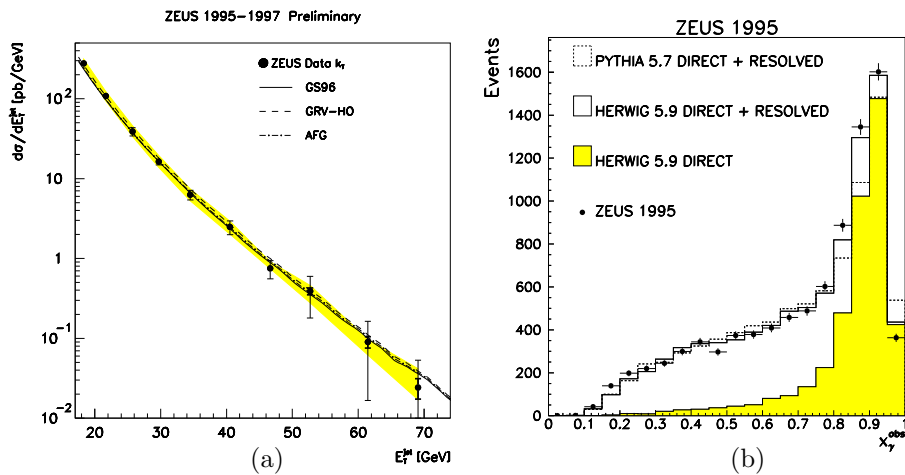


Figure 2. (a) Distribution of transverse energy of photoproduced jets in ZEUS in the pseudorapidity range $-0.75 < \eta < 2.5$. (b) Distribution of x_γ^{obs} in dijet events.

ZEUS 1996/1997 PRELIMINARY

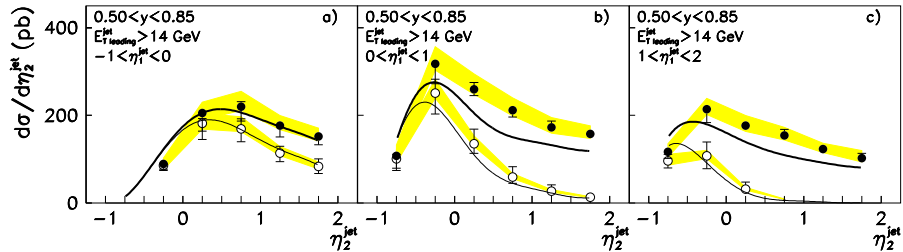


Figure 3. Cross sections for photoproduced jets, in dijet events with minimum jet E_T values of 14 GeV. The incident photon energy, as a fraction y of the e beam energy, is restricted to high values. Full circles = all x_γ^{obs} ; open circles = $x_\gamma^{obs} > 0.75$. The pseudorapidity of one jet is plotted for given intervals of that of the other. The shaded bands represent experimental uncertainty due to the simulation of the response of the ZEUS calorimeter. Uncertainties of up to 15% due to the QCD scale, and 10% due to effects of hadronisation, should be allowed on the theoretical predictions.

in order to avoid the uncertainties concerning seed definition and jet merging present with the cone algorithm approach.⁵ Figure 2(b) shows the x_γ^{obs} spectrum obtained by ZEUS using high E_T jet pairs. The shape of the distribution can be well fitted using PYTHIA and HERWIG LO simulations of the resolved and direct processes, provided that each contribution is rescaled. It is important to note that the shape of the distribution depends strongly on the cuts imposed upon the jet parameters, as will be seen below.

By selecting on $x_\gamma^{obs} < 0.75$ or $x_\gamma^{obs} > 0.75$, event samples can be obtained in which the hadronic (resolved) or pointlike (direct) photon diagrams dominate.

The availability of good jet statistics at high E_T removes most of the problems concerning a possible “underlying event”, due to multi-parton interaction effects (MI),⁶ whose presence has been postulated at lower jet energies where the low- x_γ cross sections are often higher than expected.^{5,7} Studies of the energy flow around the jets have shown that MI effects appear to be small with the harder jets of the present study, giving stronger confidence that discrepancies between the data and theory are not due to this cause. Indeed in fig. 3 it is seen that the agreement between experiment and theory is not perfect in all kinematic regions. Discrepancies are particularly evident with higher incoming photon energies and when both emerging jets are at forward η values. The existing models are unable to account for the data, and more theoretical input would appear invited.

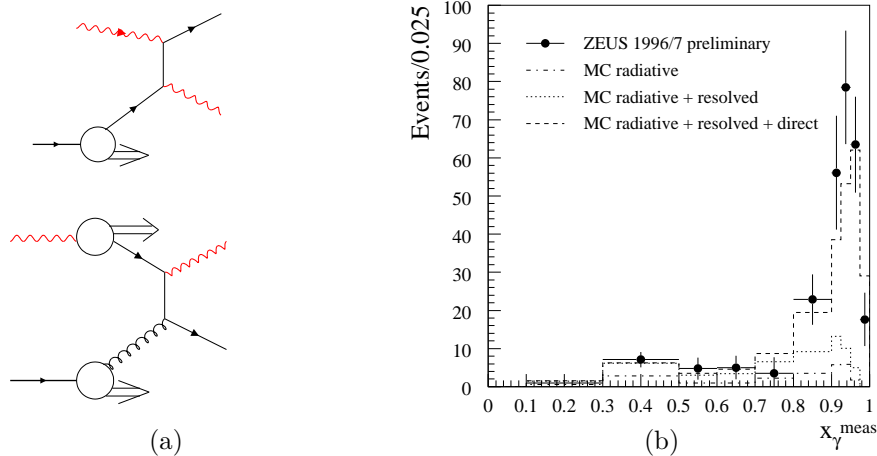


Figure 4. (a) Examples of direct and resolved LO diagrams in prompt photon photoproduction. (b) Distribution of x_γ^{meas} , defined at the detector level analogously to x_γ^{jets} , in photoproduced events having an isolated prompt photon and a jet. The photon satisfies $5 < E_T < 10$ GeV and $-0.7 < \eta < 0.9$; the jet satisfies $E_T > 4.5$ GeV and is required within a central η range. The GRV⁸ photon structure is used.

3 Prompt photon measurements.

As an alternative to jets, one can seek to measure the production of high- E_T photons, known as “prompt photons”. Since QCD processes of this type have a different set of diagrams from those of dijet processes (fig. 4(a)), they provide a complementary perspective on the physics. The photon is already a partonic object; so there are fewer complications associated with hadronisation (though a recoil jet is still present). There is less dependence on jet finding, and a photon is typically better measured than a jet. On the other hand, an important background from hard neutral mesons (mainly π^0, η) must be subtracted, and allowance must be made for photons radiated from high- E_T quarks. It is helpful to insist that the photon be isolated. ZEUS impose an isolation condition such that within a cone of unit radius in (η, ϕ) around a photon of transverse energy E_T , no more than a further $0.1E_T$ of transverse energy may be present.

When a jet is also observed, a value of x_γ may be measured from the jet and the photon. Figure 4(b) shows that the distribution is very different from that found in dijet photoproduction. The peak near unity, associated with

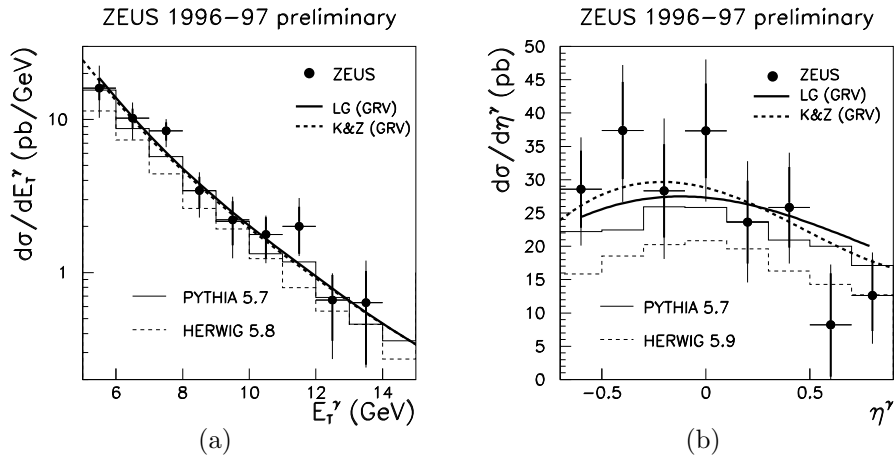


Figure 5. (a) E_T distribution of inclusive prompt photons with $-0.7 < \eta < 0.9$. (b) η distribution of inclusive prompt photons with $5 < E_T < 10$ GeV. Predictions are shown for PYTHIA 5.7, HERWIG 5.9 and two NLO calculations.^{10,11}

the direct diagrams, is considerably more pronounced than with dijets. The distribution is quite well described using PYTHIA.

Following an earlier paper on the observation of photoproduced prompt photon processes,⁹ ZEUS have presented further preliminary results. The inclusive cross section as a function of E_T is also well described by PYTHIA (fig. 5(a)) and by NLO calculations, although HERWIG appears low. Given the large errors at present, the available models describe the rapidity distributions satisfactorily (fig. 5(b)).

4 Gluon content of the photon.

The hadronic coupling of the photon has to involve charged components in the intermediate hadronic state, namely quarks – but quarks should be accompanied by a gluon component. In most models, the quarks tend to take more of the photon momentum than the gluons, so that a search for gluons in the photon should aim at a sensitivity at low x_γ values.

This is illustrated in fig. 6, which shows x_γ distributions from dijet events in H1. The shape of the distribution is changed radically when jets with lower E_T values are accepted, even while the minimum dijet mass remains at the same value. The Monte Carlo based predictions comprise components from direct processes, and from resolved processes initiated by quarks and

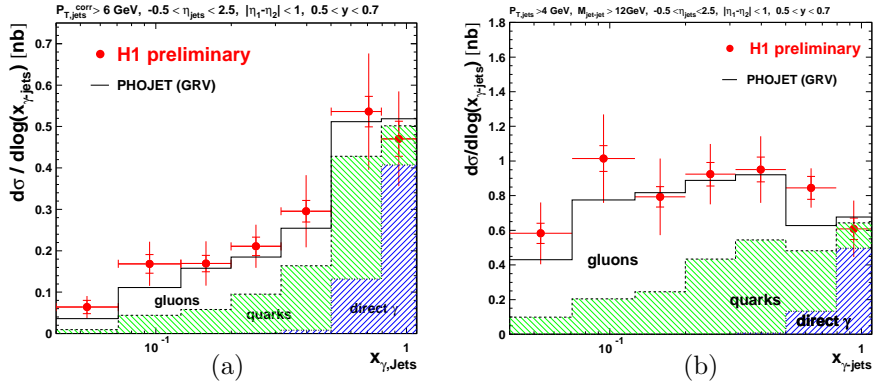


Figure 6. Plots of x_γ (H1) using dijets of mass greater than 12 GeV. In the (a), the minimum jet E_T is 6 GeV, in (b) it is 4 GeV.

by gluons within the photon. This partition of the resolved component is illustrated using the GRV photon parton densities,⁸ which have a generally good record and here too give a good fit to the data. Note that although the direct peak is no longer visible as such in (b), this is entirely a consequence of the much higher rates now obtained at lower x_γ values. Through accepting the lower- E_T jets, one has greater acceptance at low x_γ giving a greater sensitivity to the gluon. Indeed, if the quark part of the resolved photon is as modelled above, the level and shape of the cross sections already imply a quantitative observation of gluons in the photon.

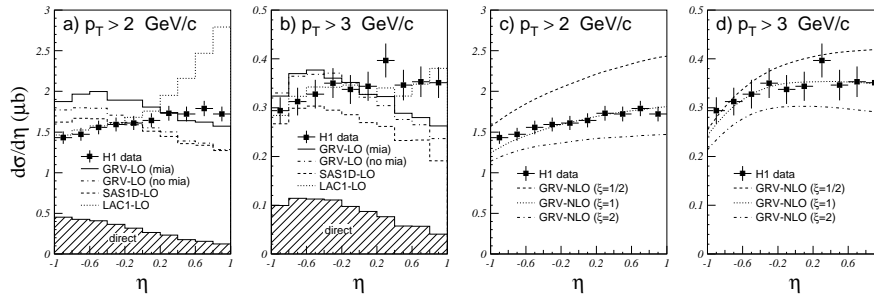


Figure 7. Distribution of inclusive charged particles measure by H1. The data are compared with (a,b) LO Monte Carlo distributions and (c,d) NLO curves.

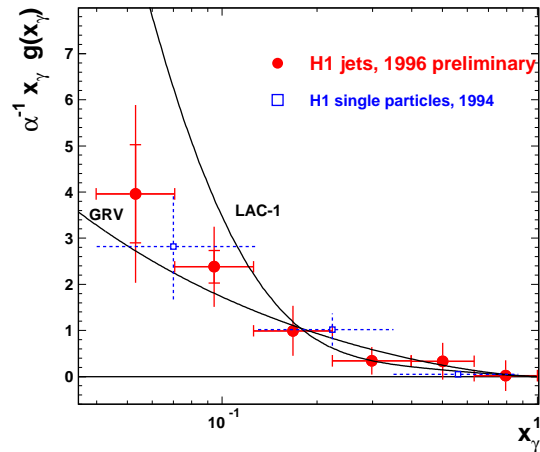


Figure 8. Gluon density in photon, as measured by H1 using inclusive tracks and dijet events. The error bars include uncertainties in the subtraction of the quark component.

A further study has now been performed by means of inclusive charged particles measured in H1.¹² Above transverse momenta of 2–3 GeV, such particles are fairly well associated with high- p_T partons; they are also well measured in the apparatus. Distributions are shown in fig. 7, where it is demonstrated that the 3 GeV data can be described by means of LO theory using a suitably chosen photon structure. NLO calculations are also successful, but there exists a large QCD scale uncertainty.

An x_γ estimator $x_\gamma^{rec} = \sum p_T e^{-\eta} / E_\gamma$ is now evaluated by summing over selected high- p_T tracks in an event. Using PYTHIA, good correlation is found between x_γ^{rec} and x_γ at the LO parton level, which permits an unfolding procedure to be used to evaluate cross sections as a function of x_γ . These are then converted to photon parton densities. Calculated quark densities in the photon are now subtracted off (with a small amount of model dependence), and one is left with a measurement of the gluon densities.

The assumption behind this procedure is that the existing photon models, based on e^+e^- collider data, have relatively well-determined quark densities. The H1 results are shown in fig. 8, together with those from a similar recent analysis which uses jets rather than charged particles. The two sets of points are consistent, and agree well with the GRV model of the photon gluon density. As is commonly the case, LAC1¹³ is too high.

5 Studies of the virtual photon

The LO differential cross section for the process $ep \rightarrow$ dijets can be written

$$\frac{d^5\sigma}{dy dx_\gamma dx_p d\cos\theta^* dQ^2} = \frac{1}{32\pi s_{ep} y x_\gamma x_p} \times \\ \times \sum f_{\gamma/e}^k(y, Q^2) f_{i/\gamma}^k(x_\gamma, P_t^2, Q^2) f_{j/p}(x_p, P_t^2) |M_{i,j}(\cos\theta^*)|^2. \quad (1)$$

The sum is over the polarisation k of the photon emitted by the electron, and the parton species i and j in the photon and the proton, respectively. The terms f denote the photon density in the electron and the parton densities in the photon and proton; $M_{i,j}$ denotes the QCD matrix element.

Within the acceptance of a typical experiment, most of the $2 \rightarrow 2$ parton processes are t -channel exchanges with similar shape. The Single Effective Subprocess approximation¹⁴ replaces all the $M_{i,j}$ terms by a common expression $M_{SES}(\cos\theta^*)$, and forms combinations \tilde{f} of the parton densities. These are known as Effective Parton Densities (EPDs). Taking into account the colour charge on the gluon, one obtains for the proton:

$$\tilde{f}_p = \sum (f_{q/p}(x_p, P_t^2) + f_{\bar{q}/p}(x_p, P_t^2)) + \frac{9}{4} f_{g/p}(x_p, P_t^2),$$

summing over quark flavours. Only transverse polarised photons are retained. Then the sum in (1) can be replaced by the single effective term:

$$f_{\gamma/e}^T(y, Q^2) \tilde{f}_\gamma(x_\gamma, P_t^2, Q^2) \tilde{f}_p(x_p, P_t^2) |M_{SES}(\cos\theta^*)|^2.$$

The SES and EPD approximations provide an experimental procedure for comparing the properties of the photon in different situations. On this basis, H1 have measured the EPD \tilde{f}_γ in the photon over a range of small to medium values of Q^2 , using photoproduced jet pairs of transverse momentum P_t .¹⁵ The aim is to examine the variation of \tilde{f}_γ with x_γ , Q^2 and P_t^2 and compare with QCD predictions.

This is a two-scale situation. It is first found that the x_γ^{jets} distributions show a clear trend, as Q^2 and P_t^2 separately increase, to be more and more dominated by the “direct peak” at $x_\gamma^{jets} \approx 1$. In other words, the hadronic properties of the photon decrease as the process becomes “harder”. Such a situation is not new and has commonly involved the employment of meson-like form factors. However the HO QCD diagrams add further complexity and interest to the present type of interaction.

Figure 9(a) shows the variation of \tilde{f}_γ with Q^2 at two x_γ values. (The variation with P_t^2 is found to be weak.) Also plotted are predictions from a pure VMD ρ -pole form factor, and modern QCD-based calculations from

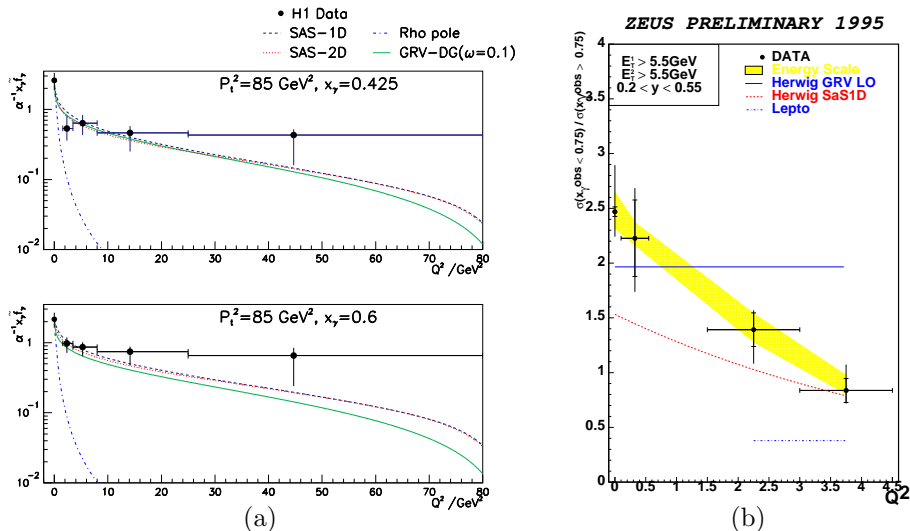


Figure 9. Q^2 dependence of (a) effective parton densities in photon (H1) and (b) ratio of low- x_γ^{obs} to high- x_γ^{obs} cross sections (ZEUS).

Schuler and Sjöstrand.¹⁶ The latter are valid only in the kinematic range $\Lambda_{QCD}^2 \ll Q^2 \ll P_t^2$. Two conclusions follow; one is that as now expected, a ρ pole form factor alone is quite insufficient. The second is that the QCD approach gives good results in the region where its validity is claimed, namely for $0.1 \ll Q^2 \ll 85 \text{ GeV}^2$ but perhaps fails elsewhere. Altogether, given the approximations made, this would seem to represent a considerable success, and confirms the H1 collaborations earlier results in terms of inclusive jets.¹⁷

Over a finer scale of low Q^2 values, however, ZEUS have shown that at present there still may be problems in describing the behaviour of the photon. Fig. 9(b) shows the cross section ratio $\sigma(x_\gamma^{obs} < 0.75) / \sigma(x_\gamma^{obs} > 0.75)$ for a kinematic range of centrally produced jet pairs. At $Q^2 \approx 0$ the lower x_γ^{obs} range is dominated by hadronic (“resolved”) diagrams. The ratio falls with Q^2 , as predicted by SaS, but the latter theory does not reproduce the magnitude of the effect. At $Q^2 \approx 0$, the data lie above the GRV prediction (which is not modelled to fall with Q^2), indicating the possible presence of multiparton interactions under these conditions. The Lepto line represents a model with no hadronic component to the photon, and NLO effects confined to parton showers; it fails completely at these Q^2 values.

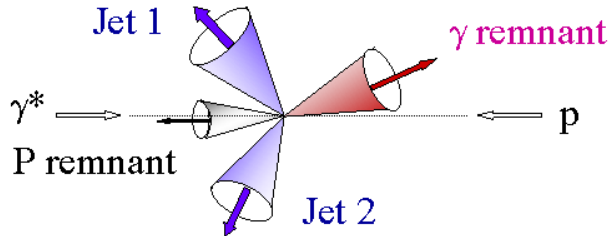


Figure 10. Event topology for photon remnant studies.

6 Study of the photon remnant.

The properties of the photon remnant offer a means for testing whether the so-called anomalous photon processes are correctly described in present theories. To achieve this, H1 have employed a customised jet finder to identify events with two high- E_T jets accompanied by a proton remnant and a photon remnant. The latter is then treated as a jet-like object whose properties can be studied. Fig. 11 shows the mean p_T of the photon remnant relative to the beam, plotted as a function of (a) the virtuality of the incident photon, and (b) the mean E_T of the two hard jets. In this way, theory can be tested over a range of kinematic parameters.

The results show that HERWIG describes the behaviour of the photon remnant quite well, apart perhaps from the case of the softest “hard” jets. An intrinsic k_T of partons within the photon of 0.66 GeV was taken. Within HERWIG, most of the transverse momentum observed at $Q^2 \approx 0$ arises from the effects of hadronisation: to study the parton level properties of the anomalous photon coupling, it may therefore be best to go to Q^2 values of more than a few GeV^2 . On the other hand, the RAPGAP Monte Carlo is not successful in this context.

7 Three-jet events in photoproduction.

With the aim of confirming our understanding of the QCD processes that are operative in the photoproduction of jets, ZEUS have performed an investigation of three-jet events in photoproduction.¹⁸ The most important experimental requirement was for the three-jet mass to exceed 50 GeV. The kinematics of the final state are best studied in the three-jet centre-of-mass frame, as illustrated in fig. 12. The angle ψ_3 is defined between the plane of the three

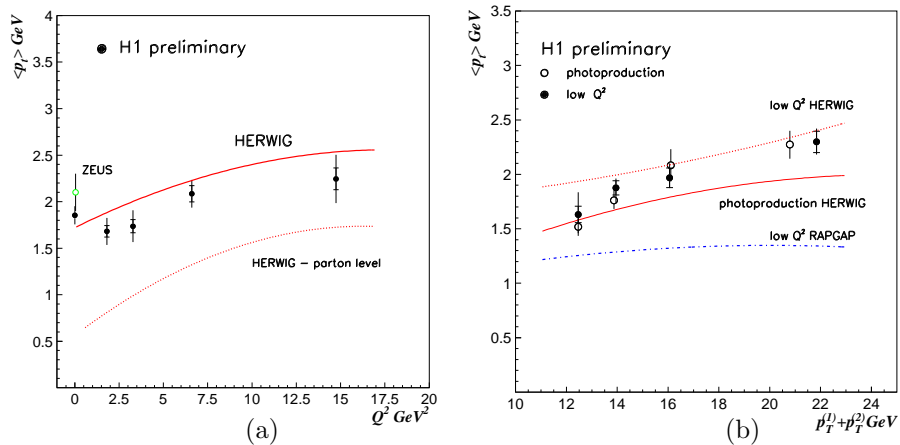


Figure 11. Variation of the mean p_T of the photon remnant (a) with the virtuality of the photon (b) with the mean transverse energy of the hard jets.

jets, and the plane containing the incident proton and photon directions and the highest- E_T jet, labelled “3”.

The distribution of ψ_3 is sensitive to a number of kinematic and dynamical properties of the process (fig. 12). It should first be noted that owing to the kinematic requirements on the jets, the distribution is depleted near zero and 180° ; what appears as a two-peaked structure would otherwise be a steep-sided valley. Likewise, the flat ψ_3 distribution that would be had if the three jets (or high- p_T partons) were produced according to phase space now becomes centrally peaked. The latter shape in no way resembles the data, confirming that dynamical mechanisms are shaping the three-jet production.

Higher-order calculations describe the shape of the observed distribution well, as indeed do HERWIG and PYTHIA. From further investigations it was found that the main contribution to the three-jet process comes from initial-state gluon radiation from the proton and photon. (The higher peak near 180° comes from the higher amount of initial-state radiation from the proton.) Final-state radiation is relatively suppressed since the third jet then needs to become substantially separated from its parent jet. It is also possible to switch off the colour coherence structures within PYTHIA. The result is a flatter ψ_3 distribution whose shape does not agree well with the data. With further statistics, one may hope to distinguish between the PYTHIA and HERWIG models and possibly some of the higher order calculations.

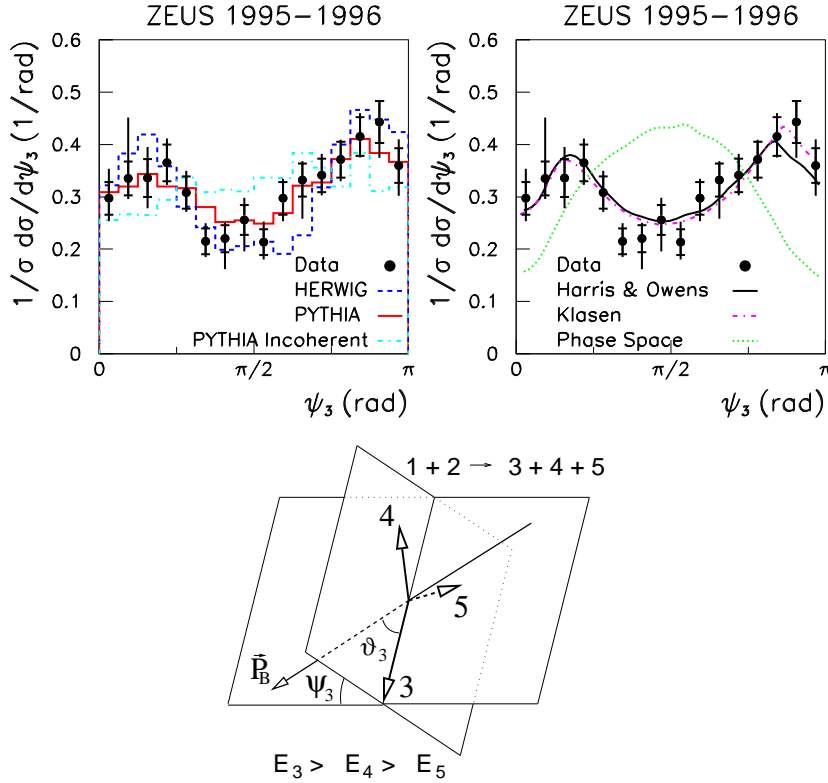


Figure 12. Definition and distribution of ψ_3 in three-jet events in photoproduction.

8 SubJets

A further useful tool for studying the parton structure of the photon would be a knowledge of the nature of a given hard jet. When a jet is due to a heavy quark, this may often be determined on a jet-by-jet basis; however the majority of jets in photoproduction are from light quarks and gluons. Studies made by ZEUS of jet widths¹⁹ have now been supplemented by studies on the numbers of “subjets” within a jet. The concept of a subjet arises in terms of clustering jet algorithms such as the k_T algorithm, where a cut y_{cut} on the clustering parameter determines whether two jet candidates shall be merged. The algorithm is iterated until all remaining pairs of jet candidates have clustering parameters above this value, which is chosen to correspond

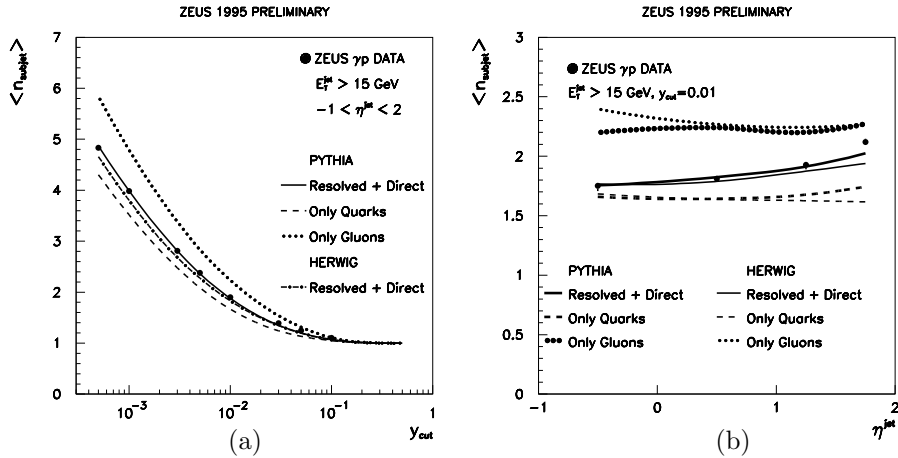


Figure 13. (a) Variation of number of subjects with cut parameter for photoproduced jets with $E_T > 15$ GeV at HERA (b) variation with pseudorapidity for fixed $y_{cut} = 0.01$. Gluon jets are predicted to have higher $\langle n_{subject} \rangle$ than quark jets.

to an acceptable overall jet radius. A large value of y_{cut} gives more merging, and fewer final jets.

Having found a jet, it is possible to rerun the algorithm using varying smaller values of y_{cut} ; a number of smaller jets (“subjects”) may now be obtained in place of the original one. This number, at given y_{cut} , is an indicator of the internal structure of the jet.

Fig. 13(a) shows the variation of the mean number of subjects $\langle n_{subject} \rangle$ with y_{cut} for photoproduced high- E_T jets in ZEUS. The form of the variation can be simulated using HERWIG and PYTHIA, and is intermediate between the expectations for pure quark-initiated and pure gluon-initiated jets, corresponding well to an appropriate mixture of direct and resolved processes.

With a chosen fixed y_{cut} value, it is then possible to study the variation of $\langle n_{subject} \rangle$ with, for example, the pseudorapidity of the primary jet, as shown in fig. 13(b). It is apparent that the jets are predominantly quarklike at negative η values but predominantly gluonlike for positive η . The variation of the data is reasonably well reproduced using the GRV photon structure. It is too early to say if this technique can prove fruitful in distinguishing between different photon models, but it is clearly a potentially useful addition to the physicist’s repertoire in an area where investigations are notoriously difficult.

9 Conclusions

HERA provides an environment in which many aspects of photon physics can be investigated. The past two years have seen a significant expansion both in the numbers of photoproduction analyses and in their scope. Studies of jet production have reached the stage where kinematic regions can be investigated where the possible complications from underlying parton-parton events should not be a problem; nevertheless, there are discrepancies even here with the present theoretical predictions, even at next-to-leading order, which seem to invite new thinking at the theoretical level. The study of prompt photons in photoproduction is now a possibility, given the present possible luminosities at HERA, and is able to provide new perspectives in the area of hard photon interactions.

The gluon content of the photon has been studied further by the extension of existing techniques. These results from H1 are consistent with the best available photon models, but the errors remain fairly large. Both H1 and ZEUS have begun to study the transition from the quasi-real photon, with its extensive hadronic properties, to the virtual state, still at moderate Q^2 values, where “anomalous” photon coupling becomes a more dominant effect, providing an perturbative QCD element in low- x_γ photon physics. New studies of the photon remnant provide further insight into the “anomalous” photon.

The actual QCD mechanisms remain an important area of study. Here, multi-jet final states and the teasing apart of jets into “subjets” have begun to give improved confirmation of our understanding of detailed aspects of the hadronic interactions initiated by a photon.

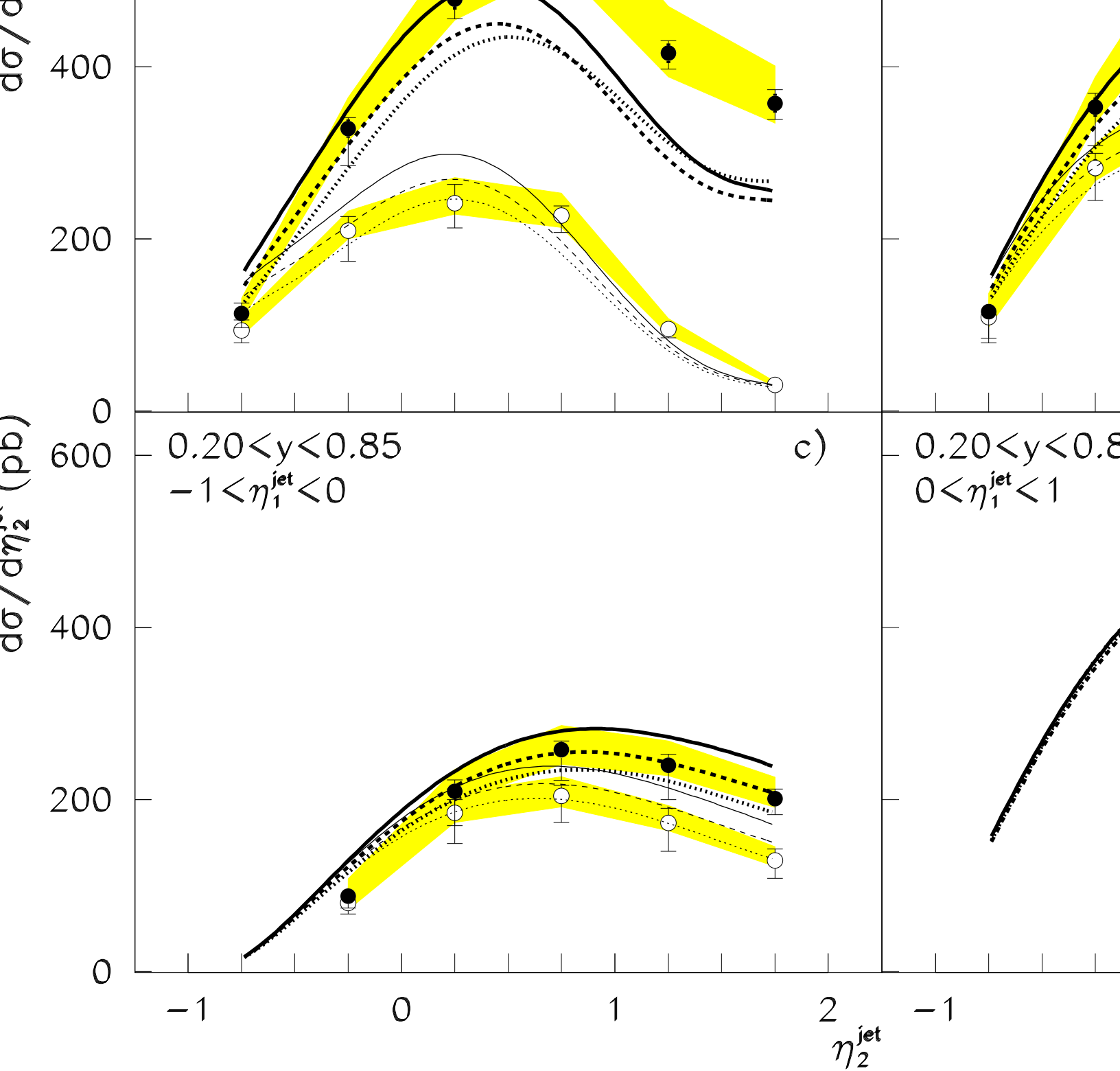
To conclude, photon physics at HERA has entered a new and remarkably productive stage. The entire area of heavy flavour production was omitted here, being part of another speaker’s remit! There are still many avenues to investigate and many questions to answer. The future at HERA will hopefully provide us with the opportunity to unravel further the properties of a particle, the photon, which proves to have a richer and more complex nature the more it is examined.

Acknowledgments

The author wishes to thank members of the H1 and ZEUS collaborations for much helpful information in the preparation of this talk, and also the Royal Society (London) for financial assistance in attending the Conference.

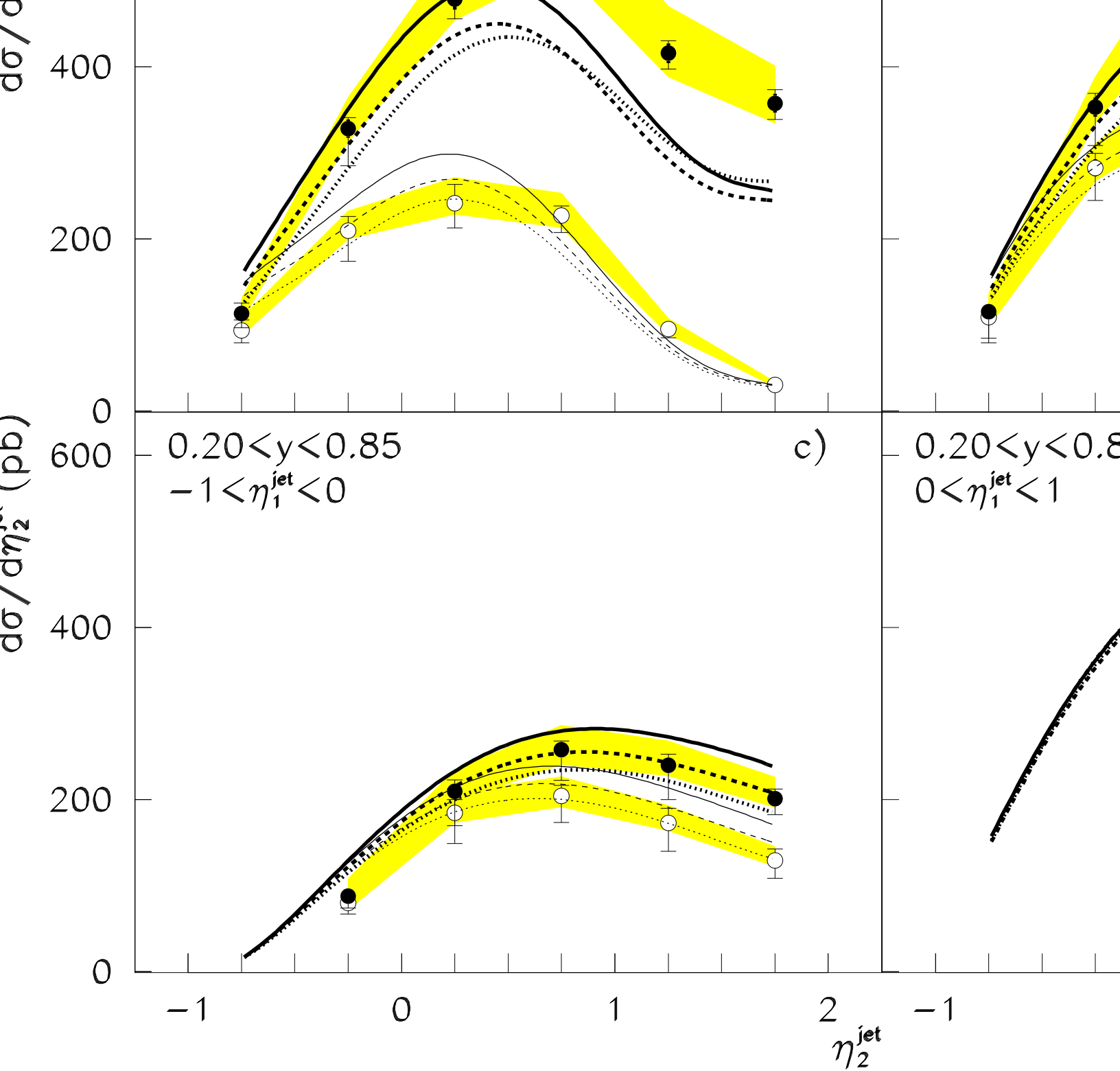
References

1. G A Schuler and T Sjöstrand, Nucl. Phys. **B 407**, 539 (1993);
G A Schuler and T Sjöstrand, *Phys. Lett. B* **300**, 169 (1993).
2. ZEUS Collab., J. Breitweg et al., DESY 99-057, subm. to Eur. Phys. J. C.
3. P Aurenche et al., proceedings, *Future Physics at HERA*, eds. G. Ingelman et al., DESY (1996) 570;
S Frixione and G Ridolfi, Nucl. Phys. **B 507**, 315 (1997);
B Harris and J Owens, *Phys. Rev. D* **57**, 5555 (1998);
M Klasen, T Kleinwort and G Kramer, Eur. Phys. J. **C1**, 1 (1998).
4. S. Catani et al., Nucl. Phys. **B 406**, 1993 (187).
5. ZEUS Collab., J. Breitweg et al., Eur. Phys. J. **C1**, 109 (1998).
6. J. M. Butterworth et al., J. Phys. **G 22**, 883 (1996).
7. H1 Collab., S. Aid et al., Z. Phys. **C 70**, 17 (1996).
8. M. Glück, E. Reya and A. Vogt, Phys. Rev. **D46**, 1973 (1992).
9. ZEUS Collab., J. Breitweg et al., *Phys. Lett. B* **413**, 201 (1997).
10. M. Krawczyk and A. Zembruski, proc. *ICHEP'98*, Vancouver, eds. A. Astbury, D. Axen and J. Robinson, (World Scientific, Singapore, 1999), 895 and hep-ph/9810253.
11. L. E. Gordon, Phys. Rev. **D57**, 235 (1998) and private communication;
L. E. Gordon, proceedings, *Photon 97*, Egmond aan Zee, eds. A. Buijs and F. Ern  (World Scientific, Singapore, 1998), 173 and hep-ph/9706355.
12. H1 Collab., C. Adloff et al., DESY 98-148, to appear in Eur. Phys. J. C.
13. H. Abramowicz, K. Charchuła and A. Levy, PLB **269**, 458 (1991).
14. B. V. Combridge and C. J. Maxwell, Nucl. Phys. **B 239**, 429 (1984).
15. H1 Collab., C. Adloff et al., EJP **C 1**, 97 (1998);
H1 Collab., C. Adloff et al., DESY 98-205, to appear in Eur. Phys. J. C.
16. G. A. Schuler and T Sjöstrand, *Phys. Lett. B* **376**, 1973 (1996).
17. C. Adloff et al., PLB **415**, 418 (1997).
18. ZEUS Collab., J. Breitweg et al., *Phys. Lett. B* **443**, 394 (1998).
19. ZEUS Collab., J. Breitweg et al., Eur. Phys. J. **C 8**, 367 (1999).



Figures a), b) and c):

- | | |
|--------------------|--|
| ● ZEUS 1995 | ○ ZEUS 1995, $x_\gamma^{\text{obs}} > 0.75$ |
| — NLO-QCD, GRV-HO | — NLO-QCD, GRV-HO, $x_\gamma^{\text{obs}} > 0.75$ |
| ⋯ NLO-QCD, AFG-HO | ⋯ NLO-QCD, AFG-HO, $x_\gamma^{\text{obs}} > 0.75$ |
| ⋯ NLO-QCD, GS96-HO | ⋯ NLO-QCD, GS96-HO, $x_\gamma^{\text{obs}} > 0.75$ |



Figures a), b) and c):

- | | |
|--------------------|--|
| ● ZEUS 1995 | ○ ZEUS 1995, $x_\gamma^{\text{obs}} > 0.75$ |
| — NLO-QCD, GRV-HO | — NLO-QCD, GRV-HO, $x_\gamma^{\text{obs}} > 0.75$ |
| ⋯ NLO-QCD, AFG-HO | ⋯ NLO-QCD, AFG-HO, $x_\gamma^{\text{obs}} > 0.75$ |
| ⋯ NLO-QCD, GS96-HO | ⋯ NLO-QCD, GS96-HO, $x_\gamma^{\text{obs}} > 0.75$ |